

Accepted Manuscript

Title: Phosphotungstic acid supported on silica-coated CoFe₂O₄ nanoparticles: An efficient and magnetically-recoverable catalyst for *N*-formylation of amines under solvent-free conditions

Author: M. Kooti E. Nasiri

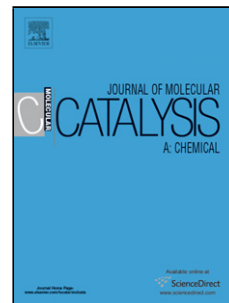
PII: S1381-1169(15)00182-X
DOI: <http://dx.doi.org/doi:10.1016/j.molcata.2015.05.009>
Reference: MOLCAA 9495

To appear in: *Journal of Molecular Catalysis A: Chemical*

Received date: 21-12-2014
Revised date: 29-4-2015
Accepted date: 14-5-2015

Please cite this article as: M.Kooti, E.Nasiri, Phosphotungstic acid supported on silica-coated CoFe₂O₄ nanoparticles: An efficient and magnetically-recoverable catalyst for *N*-formylation of amines under solvent-free conditions, *Journal of Molecular Catalysis A: Chemical* <http://dx.doi.org/10.1016/j.molcata.2015.05.009>

This is a PDF file of an unedited manuscript that has been accepted for publication. As a service to our customers we are providing this early version of the manuscript. The manuscript will undergo copyediting, typesetting, and review of the resulting proof before it is published in its final form. Please note that during the production process errors may be discovered which could affect the content, and all legal disclaimers that apply to the journal pertain.



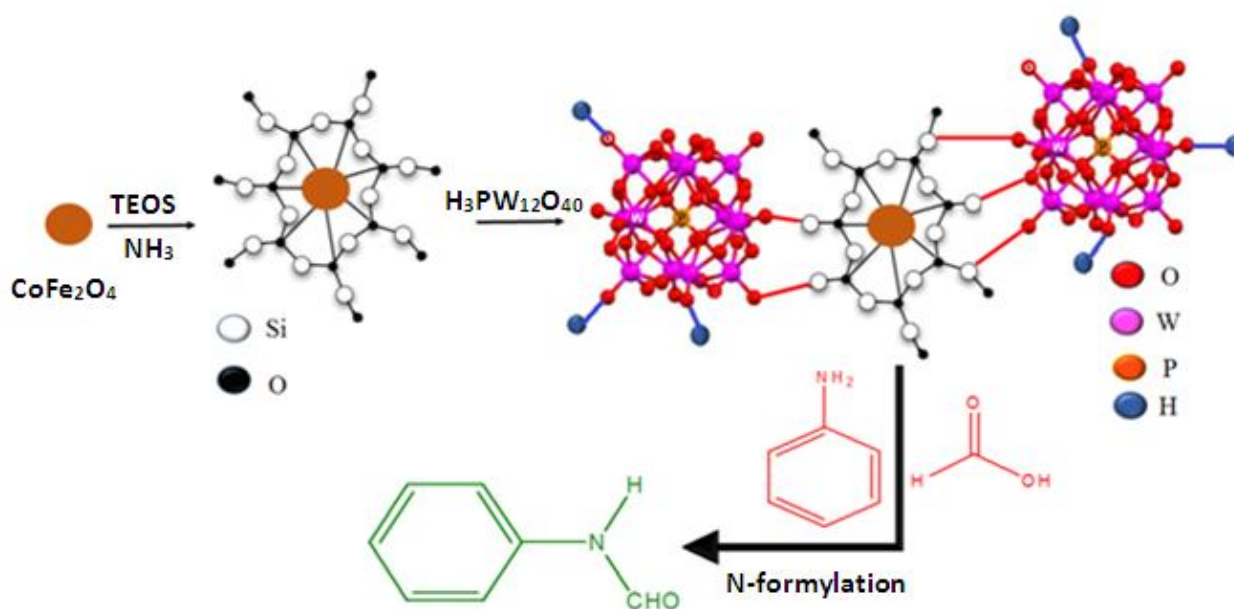
Phosphotungstic acid supported on silica-coated CoFe_2O_4 nanoparticles:
An efficient and magnetically-recoverable catalyst for N-formylation of
amines under solvent-free conditions

M. Kooti* and E. Nasiri

Department of Chemistry, Shahid Chamran University, Ahvaz, Iran

*m_kooti@scu.ac.ir

Graphical abstract



Highlights

- Phosphotungstic acid was anchored on $\text{CoFe}_2\text{O}_4@\text{SiO}_2$.
- This composite was used as catalyst in N-formylation reactions.
- The N-formylation reactions were carried out under solventless conditions.
- The catalyst can be recovered by applying a permanent magnet.

Abstract

Phosphotungstic acid (PTA) was rapidly and efficiently anchored on the surface of silica coated cobalt ferrite core to obtain a new three-component $\text{CoFe}_2\text{O}_4@\text{SiO}_2\text{-PTA}$ nanocomposite. The resultant composite was characterized by various techniques, including FT-IR, XRD, SEM, EDX, ICP-AES, and VSM. The as-synthesized nanocomposite was examined as catalyst for N-formylation of various amines under solvent-free conditions at room temperature. Due to the presence of magnetic core in this catalyst, it can be easily separated from the reaction media by applying an external magnetic field. The isolated catalyst can be reused for at least five successive times without significant leaching or loss of its high catalytic activity.

Keywords: Phosphotungstic acid; Aniline; Nanocomposite; Cobalt ferrite; N-formylation.

1. Introduction

Heteropolyacids, with the molecular formula of $[\text{XM}_{12}\text{O}_{40}]^{n-}$, where $\text{X} = \text{P}^{5+}$, As^{5+} , Si^{4+} , or Ge^{4+} and $\text{M} = \text{Mo}^{6+}$, or W^{6+} , have been extensively used as catalysts for various organic reactions due to their unique physicochemical properties [1-6]. Among the well-known Keggin types of these solid acids, phosphotungstic acid (PTA), $\text{H}_3\text{PW}_{12}\text{O}_{40}$, has been the target catalyst and received considerable attention in the last decade because of its super strong Brønsted acidity as well as its ease of preparation [7-9]. It is well documented that immobilization of PTA on a suitable support can eliminate its encountered major drawbacks, namely, (i) very low surface area, and (ii) instability in polar solvents. In fact, most of the acidic protons of the bulk phosphotungstic acid are in the interior of the solid which are inaccessible for catalysis of non-polar hydrocarbon reactions. Supported PTA, however, has a

greater number of surface acid sites than its bulk component and therefore presents higher catalytic activity [10-13].

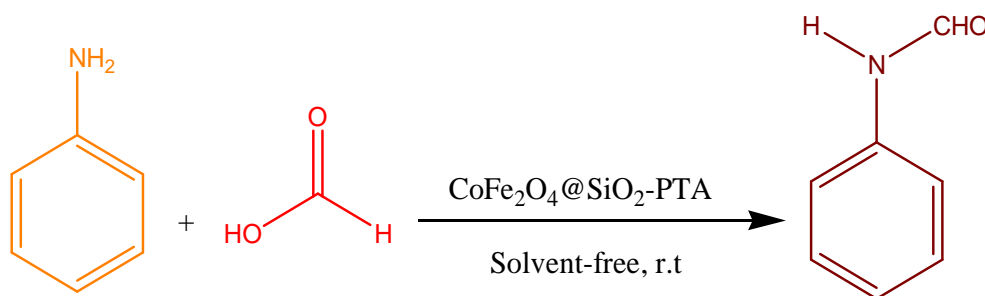
Various materials, especially mesoporous type, have been used as support for PTA, such as, silica, activated carbon, zeolites, alumina, zirconia, titania and etc. [14-18]. Out of these materials, silica (SiO_2) is the most appealing support for PTA due to its relative ease of preparation, hydrophilic nature, non-basic character, physical and chemical stability and good biocompatibility [19,20]. While PTA supported on silica shows high catalytic efficiency and can be recycled more readily than its homogeneous counterpart, the tedious recovery procedure via filtration or centrifugation and the inevitable loss of the solid catalyst in the separation process still limited its application especially for the small nanosized particles. Introducing magnetic nanoparticles (MNPs) into the PTA supported silica can provide a means for efficient separation of the catalyst from reaction media. Therefore, MNPs based catalysts have been recently receiving growing attention, as they can be easily separated from the reaction mixture by applying a simple permanent magnet [21-24]. The approach of magnetic separation, taking advantage of MNPs, is typically more effective than filtration or centrifugation as it prevents loss of the catalyst into the environment.

Although there are many types of MNPs, spinel ferrites with the general formula of MFe_2O_4 (M is a divalent metal like Co^{2+} , Ni^{2+} and etc.) show interesting properties and have potential applications in various fields [25-27]. Among several spinel ferrites, cobalt ferrite (CoFe_2O_4) has gained a great deal of attention because of its high thermal stability, moderate saturation magnetization, remarkable chemical stability and mechanical hardness [28,29]. Coating of CoFe_2O_4 nanoparticles with silica to obtain $\text{CoFe}_2\text{O}_4@\text{SiO}_2$ composite, will achieve further stabilization of these MNPs as well as prevents their agglomeration in solution. The outer mesoporous silica shell of $\text{CoFe}_2\text{O}_4@\text{SiO}_2$ composite, with core-shell

structure, makes it suitable for multifunctional surface modification such as catalyst immobilization [30-34].

Phosphotungstic acid can catalyze many organic reactions requiring acid sites. One of these reactions is N-formylation of amines, which generally leads to the formation of formamides. This is an important organic reaction since formamides are intermediates in the synthesis of various heterocyclic medicinally useful compounds. Although several methods have been so far used for achieving formylation of amines, most of these methods suffer from some disadvantages, including strict anhydrous conditions, low yields, long reaction times, high reaction temperature, expensive and toxic reagents, use of harmful solvents, and etc. [35-40].

In continuation of our previous works on the development of non-toxic, low cost, eco-friendly and easily recyclable catalysts [41,42], we herein report the preparation of a new three-component $\text{CoFe}_2\text{O}_4@\text{SiO}_2\text{-PTA}$ nanocomposite via a straightforward procedure. The as-synthesized composite is consisted of a magnetically responsive CoFe_2O_4 core, silica as inner shell and PTA as outer shell. A pre-synthesized CoFe_2O_4 sample was first prepared which was then coated with silica layer and finally PTA was anchored onto the surface of the silica shell. After preparation and characterization of the new $\text{CoFe}_2\text{O}_4@\text{SiO}_2\text{-PTA}$ composite, it was used as efficient reusable, and green catalyst for some N-formylation reactions under solvent-free conditions (see Scheme 1). Within the limit of our knowledge, this is the first example of using PTA supported on silica-coated CoFe_2O_4 as efficient catalyst for N-formylation process.



Scheme 1. N-formylation of amine in the presence of $\text{CoFe}_2\text{O}_4@\text{SiO}_2\text{-PTA}$.

2. Experimental

2.1. Materials and methods

All the chemicals were of analytical grade and used without further purification.

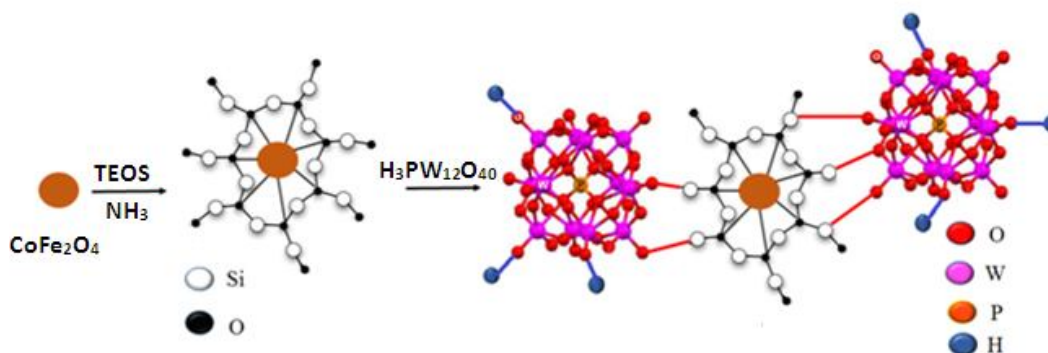
Manipulation and reactions were carried out in air without the protection of inert gas.

Phosphotungstic acid was synthesized according to the literature [43]. Fourier transform infrared (FT-IR) spectra were obtained using a FT BOMEM MB102 spectrophotometer. X-ray diffraction (XRD) patterns of the synthesized samples were taken with a Philips X-ray diffractometer (model PW1840) over a 2θ range from 10 to 80° using $\text{Cu K}\alpha$ radiation ($\lambda=1.54056 \text{ \AA}$). The FESEM images were obtained using a Hitachi Japan S4160 scanning electron microscope. The magnetic properties of the fabricated $\text{CoFe}_2\text{O}_4@\text{SiO}_2\text{-PTA}$ composite as well as other samples were studied using vibrating sample magnetometer (VSM) of Meghnatis DaghighKavir Company.

2.2. Synthesis of $\text{CoFe}_2\text{O}_4@\text{SiO}_2\text{-PTA}$ nanocomposite

Cobalt ferrite MNPs were prepared using the method reported by Maaz et al. with some minor modification [44]. In our procedure of synthesizing CoFe_2O_4 nanoparticles, olive oil was used as surfactant instead of oleic acid. No heat treatment is required in this method and the ferrite can be easily and rapidly separated from reaction mixture using a permanent magnet. Coating of CoFe_2O_4 nanoparticles with a layer of silica was achieved through Stöber method [45], which includes hydrolysis of tetraethylorthosilicate (TEOS) in the presence of NH_3 to obtain the two-component $\text{CoFe}_2\text{O}_4@\text{SiO}_2$ composite. The latter composite was

collected by applying a permanent magnet and was finely powdered after being dried. The surface of the as-fabricated $\text{CoFe}_2\text{O}_4@\text{SiO}_2$ composite was then anchored with PTA via a simple procedure. In this procedure, a round-bottom flask was charged with ethanol-water (80:20 ratio) solution containing 1.0 g of PTA and the solution was stirred at room temperature for 1 h. Into this solution, 1.0 g of $\text{CoFe}_2\text{O}_4@\text{SiO}_2$ was dispersed and stirring was continued for additional 3 h. The resulting final solid was separated by magnetic decantation, washed with cold absolute ethanol and dried in an oven at 100 °C for 2 h. The amount of PTA in $\text{CoFe}_2\text{O}_4@\text{SiO}_2$ -PTA composite was found to be 0.0875 mmol g⁻¹, as determined by ICP-AES analysis. The amount of H⁺ in the $\text{CoFe}_2\text{O}_4@\text{SiO}_2$ -PPA, determined by acid-base titration, was 0.10 mmol/g. The step-by-step fabrication of the composite ($\text{CoFe}_2\text{O}_4@\text{SiO}_2$ -PTA) is shown in Scheme 2.



Scheme 2. Step - by- step synthesis of $\text{CoFe}_2\text{O}_4@\text{SiO}_2$ -PTA nanocomposite.

2.3. General procedure for N-formylation reactions catalyzed by $\text{CoFe}_2\text{O}_4@\text{SiO}_2$ -PTA under solvent-free conditions

A mixture of aniline (1.0 mmol), formic acid (1.0 mmol), and $\text{CoFe}_2\text{O}_4@\text{SiO}_2$ -PTA (0.05 g) was stirred at room temperature. The progress of the reaction was continuously monitored by TLC. After 30 m period of time and upon completion of the reaction, as indicated by TLC tests, ethyl acetate was added to the reaction mixture. The catalyst was magnetically fixed at

the side wall of the reactor and the liquid phase was decanted. The catalyst was then washed with ethyl acetate and dried to be reused in a new N-formylation reaction. The isolated organic phase was washed with a saturated solution of NaHCO₃ and dried over anhydrous Na₂SO₄. The solvent, ethyl acetate, was removed by a rotary evaporator and the resulted residue was then subjected to recrystallization to obtain pure formamide product with 95% yield. Characterization of the N-formylated products, as well as determination of the yields, in this and other similar reactions were achieved by GC analysis. To further confirm the identity of the products, their physical and FT-IR spectral data were compared with those reported in the literature.

The obtained products from selected reactions of aniline derivatives with formic acid were also characterized by ¹H NMR and GC-MS techniques. The obtained analysis data, which are given below, clearly confirmed the structure and formula of the expected formamide products.

Selected spectroscopic data

N-Phenyl formamide(Entry 1)

¹H NMR (CDCl₃, 250 MHz): δ 7.1, 7.5 (m; cis and trans, para, meta and ortho Ar-H), 7.8 (s, broad, cis, NH), 8.3 (s, cis, CHO), 8.7 (d, trans, CHO), 8.8 (s, broad, trans, NH).

EI-MS: m/z = 121.2(M⁺).

N-(4-Nitrophenyl) formamide (Entry 4)

¹H NMR (CDCl₃, 250 MHz: δ 6.57–8.24 (m, Ar-H), 10.83 (s, CHO, trans), 10.74 (s, broad, trans, NH), 9.04 (s, broad, NH, cis), 8.40 (s, CHO, cis).

N-(4-cyanophenyl) formamide (Entry 5)

¹H NMR (CDCl₃, 250 MHz: δ 10.83 (s, CHO, trans), 10.74 (s, broad, trans, NH), 9.04 (s, broad, NH, cis), 8.40 (s, CHO, cis), 6.57-8.24 (m, Ar-H). EI-MS: m/z = 146.1(M⁺).

N-(4-Methoxyphenyl) formamide (Entry 8)

^1H NMR (CDCl_3 , 250 MHz): δ 6.86-6.91 (m, Ar-H), δ 8.47-8.51 (d, CHO, cis), 8.34 (s, CHO, trans), 7.43-7.46 (d, NH, trans), 7.01-7.04 (d, NH, cis), 3.80 (s, CH_3).

N-(2,5-Dimethylphenyl)formamide (Entry 9)

EI-MS: $m/z = 149.5(\text{M}^+)$.

N-benzyl formamide (Entry 10)

EI-MS: $m/z = 135.3(\text{M}^+)$.

N,N'-benzene-1,2-diylldiformamide (Entry 11)

EI-MS: $m/z = 164.4(\text{M}^+)$.

3. Results and discussion

3.1. Characterization of $\text{CoFe}_2\text{O}_4@\text{SiO}_2$ -PTA composite

The nanocomposite $\text{CoFe}_2\text{O}_4@\text{SiO}_2$ -PTA was fabricated via a straightforward three-step procedure. Cobalt ferrite, as magnetic core of the composite, was made by co-precipitation method which was then coated with a thin layer of silica. In the final step PTA was immobilized onto the surface of the silica shell.

The as-synthesized nanocomposite was characterized by various techniques. The FT-IR spectra of all synthesized samples along with pure PTA are presented in Fig. 1. As it is seen in Fig. 1-B, the FT-IR spectrum of $\text{CoFe}_2\text{O}_4@\text{SiO}_2$ -PTA contains all the characteristic peaks of its three components, i.e. CoFe_2O_4 , SiO_2 and PTA. Two peaks at 425 cm^{-1} and 588 cm^{-1} are attributed to Fe-O stretching in the tetrahedral and octahedral sites of CoFe_2O_4 respectively [46]. The bands located at 1091 cm^{-1} and 798 cm^{-1} , in the spectrum of $\text{CoFe}_2\text{O}_4@\text{SiO}_2$ composite, are ascribed to the symmetrical and asymmetrical vibration

modes of the Si–O–Si bonds in SiO₂ (see Fig.1-B) [47]. Both these peaks, with some shift due to the presence of PTA, are clearly seen in Fig. 1-B of CoFe₂O₄@SiO₂-PTA. Two other bands at 890 cm⁻¹ and 959 cm⁻¹ are also observed in the spectrum of this composite, which are respectively attributed to W–O–W and W=O stretching modes of PTA [48]. In all these samples the band centered at about 1630 cm⁻¹ is assigned to the H–O–H bending vibration of the absorbed water.

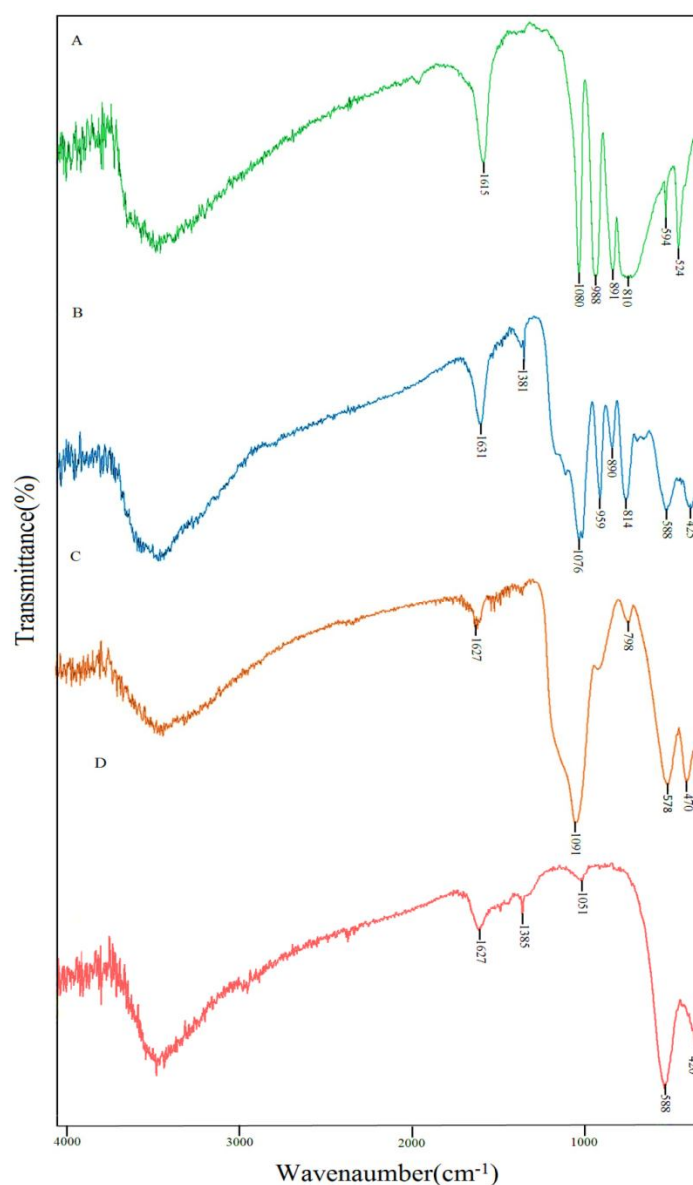


Fig. 1. FT-IR spectra of PTA(A), CoFe₂O₄@SiO₂-PTA(B), CoFe₂O₄@SiO₂(C) and CoFe₂O₄(D).

The XRD patterns of CoFe₂O₄, CoFe₂O₄@SiO₂, CoFe₂O₄@SiO₂-PTA, and free PTA are displayed in Fig. 2. The diffraction peaks related to Bragg's reflections from (2 2 0), (3 1

1), (4 0 0), (4 2 2), (5 1 1) and (4 4 0) planes correspond to the standard spinel structure of CoFe_2O_4 (JCPDS card no. 22-1086) with a space group of $Fd3m$ (see Fig. 2-A). The crystallite size of CoFe_2O_4 nanoparticles was about 18 nm, as measured by using the well-known Debye-Scherrer formula [49]. The XRD patterns of CoFe_2O_4 core, after coating with silica and anchoring with PTA (Fig. 2-B, and 2-C), are more or less the same as pristine CoFe_2O_4 revealing that the spinel cubic structure of the ferrite is retained. In the XRD patterns of the as-made $\text{CoFe}_2\text{O}_4@\text{SiO}_2$ -PTA composite, however, no crystalline phase for the immobilized PTA was observed which implied that PTA is homogeneously distributed onto the support in a non-crystalline form or that crystallites are too small. The later specificity is of importance for the catalytic properties of the synthesized composite as accessibility of the active species on the surface would be enhanced [50,51]. The lack of observing the peaks of PTA in the XRD of $\text{CoFe}_2\text{O}_4@\text{SiO}_2$ -PTA may be also due to the change in its crystal structure after immobilization.

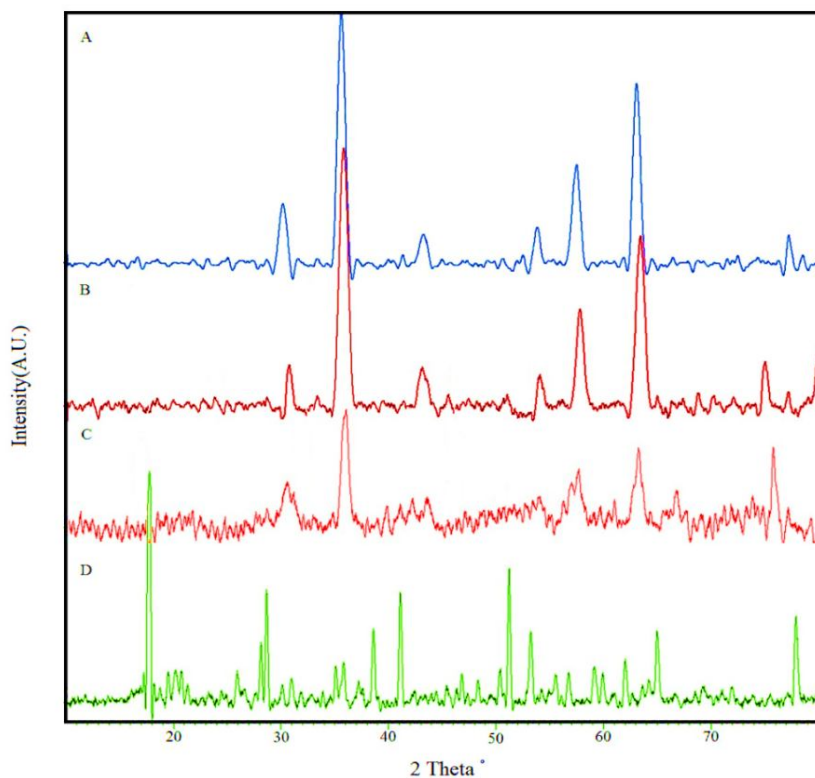


Fig. 2. XRD patterns of CoFe_2O_4 (A), $\text{CoFe}_2\text{O}_4@\text{SiO}_2$ (B), $\text{CoFe}_2\text{O}_4@\text{SiO}_2$ -PTA(C) and PTA(D).

The SEM images of CoFe_2O_4 , $\text{CoFe}_2\text{O}_4@\text{SiO}_2$ and $\text{CoFe}_2\text{O}_4@\text{SiO}_2\text{-PTA}$ are depicted in Fig. 3. As it is clearly seen, the CoFe_2O_4 and $\text{CoFe}_2\text{O}_4@\text{SiO}_2$ particles are well-resolved

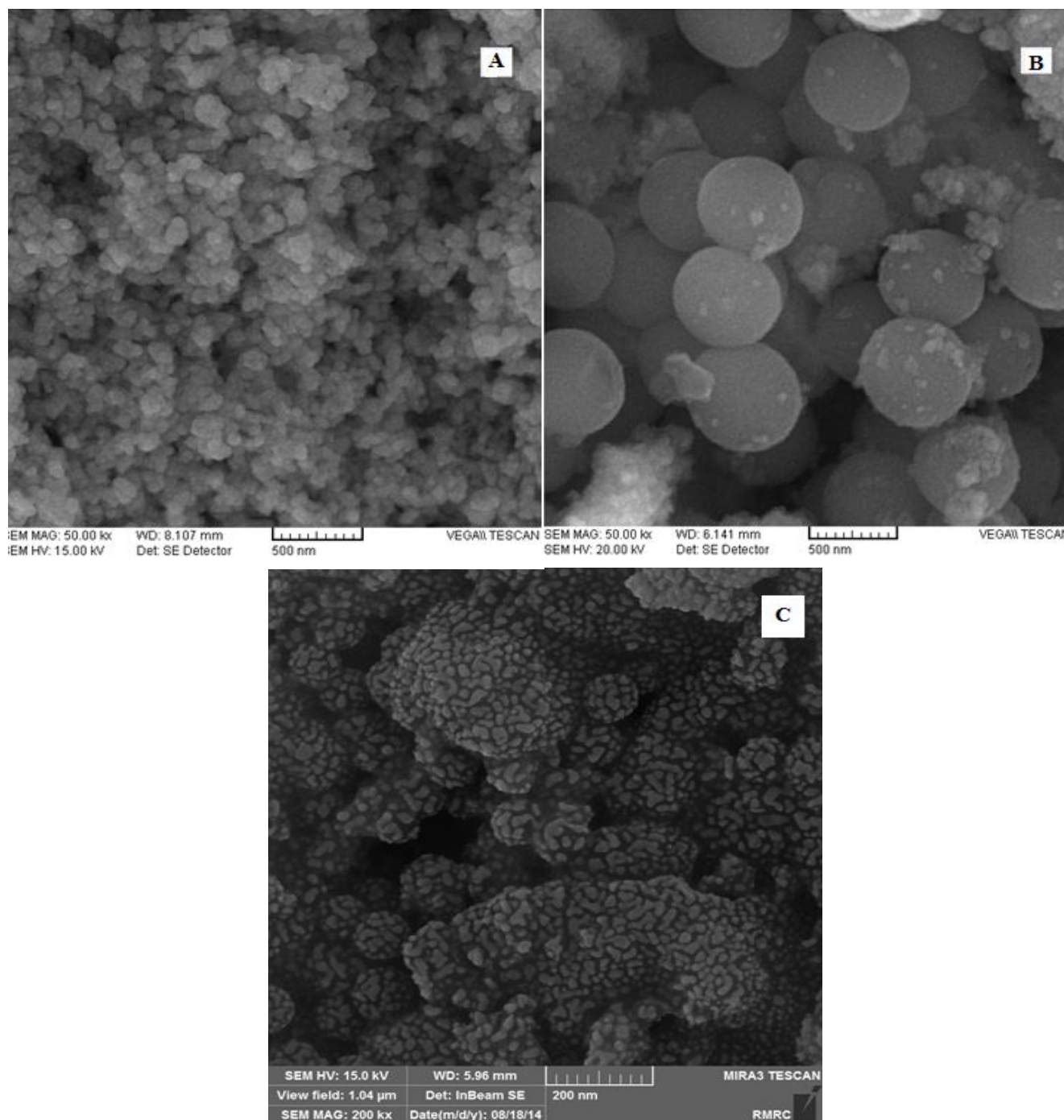


Fig. 3. SEM image of CoFe_2O_4 (A), $\text{CoFe}_2\text{O}_4@\text{SiO}_2$ (B), $\text{CoFe}_2\text{O}_4@\text{SiO}_2\text{-PTA}$ (C).

and have spherical shapes (Fig. 3-A and 3-B). The PTA particles in the SEM of $\text{CoFe}_2\text{O}_4@\text{SiO}_2\text{-PTA}$ are seen as white spots randomly inlaid on the surface of

CoFe₂O₄@SiO₂ (see Fig. 3-C). In order to further confirm the composition of the as-fabricated CoFe₂O₄@SiO₂-PTA composite, energy dispersive X-Ray (EDX) analysis was conducted. The EDX spectrum, which is displayed in Fig. 4, clearly reveals the presence of all the expected main elements (O, Si, P, Fe, Co and W) comprising this three-component composite. The surface area of CoFe₂O₄@SiO₂-PTA was also determined using the nitrogen gas adsorption (BET) method and a value of 6 m² g⁻¹ was found for this composite.

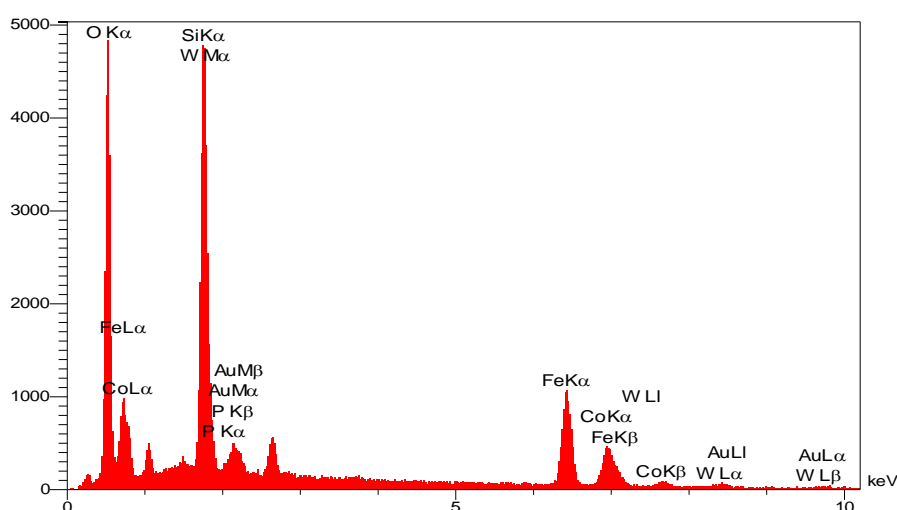


Fig. 4. EDX spectrum of CoFe₂O₄@SiO₂-PTA nanocomposite.

Magnetic measurements for CoFe₂O₄, CoFe₂O₄@SiO₂ and CoFe₂O₄@SiO₂-PTA samples were carried out using a vibrating sample magnetometer (VSM) with a peak field of 8 kOe and their hysteresis curves are shown in Fig. 5. It is clear from the hysteresis loops that the saturation magnetization (M_s) of CoFe₂O₄, CoFe₂O₄@SiO₂ and CoFe₂O₄@SiO₂-PTA are 61.05, 26.22 and 16.60 emu/g, respectively. The decrease in mass saturation magnetization in the last two composites can be attributed to the contribution of the non-magnetic silica shell and functionalized phosphotungstic acid. In fact, silica shell which surrounds the magnetic CoFe₂O₄ cores, will prevent them from approaching each other and therefore decreases the interactions between these cores [52,53]. Although the value of M_s for CoFe₂O₄ core is evidently decreased after coating with silica and anchoring with PTA, the CoFe₂O₄@SiO₂-

PTA composite, can still be efficiently and easily separated from solution with the help of an external magnetic force.

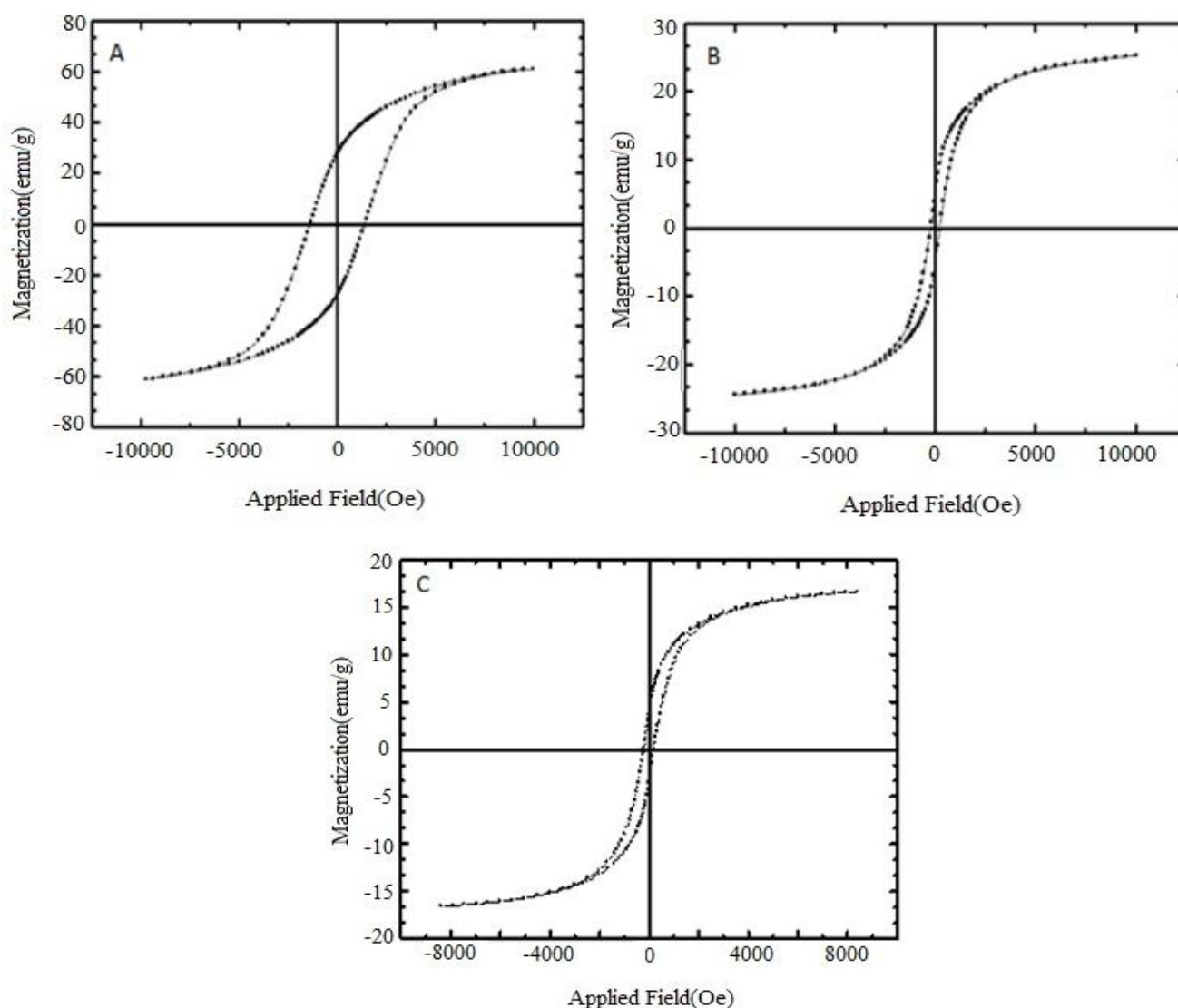


Fig. 5. Hysteresis loops of CoFe₂O₄ (A), CoFe₂O₄@SiO₂ (B) and CoFe₂O₄@SiO₂-PTA (C).

3.2. Evaluation of catalytic activity of CoFe₂O₄@SiO₂-PTA in N-formylation reactions

The reaction of aniline and formic acid was chosen as a model of N-formylation reaction. In an experiment, this reaction was carried out in the absence of CoFe₂O₄@SiO₂-PTA under solvent-free conditions. No change in the starting materials was observed after stirring the mixture at room temperature for 3 h. However, addition of a catalytic amount of

CoFe₂O₄@SiO₂-PTA to this mixture has rapidly induced N-formylation to produce formamide in high yield. This clearly reveals that this reaction can only take place in the presence of catalyst. In order to further investigate the scope and limitations of the as-prepared catalyst, different aniline derivatives and formic acid were subjected to N-formylation reaction under the same conditions and the obtained results are summarized in Table 1.

It is evident from the data in Table 1 that all examined reactions proceeded rapidly and cleanly, irrespective of the substituent types. The conversions were nearly completed within 30-60 min at room temperature and no undesirable side-reactions were observed. The difference in the yields of the corresponding N-formamides for the examined aniline derivatives is not significant. However, the observed minor differences in the obtained yields can be attributed to the change in aniline substituents i.e., anilines with electron-donating substituents, such as CH₃ and OCH₃ (Table 1; entries 8 and 9) proceed somewhat more efficiently than those having electron-withdrawing groups like Cl or NO₂ (Table 1; entries 4 and 6). The observed results of this work are in accordance with other previously reported finding [54, 55]. Interestingly, no reaction was observed with phenols (Table 1; entries 15 and 16) using the same conditions applied for N-formylation reactions. Moreover, when a molecule containing both hydroxyl and amino group was treated with formic acid, under the present reaction conditions, only N-formylated product was obtained and the OH group remained intact (Table 1; entry 14). This fact that no O-formylation was observed for phenols and aminophenol clearly conform the chemoselectivity of these reactions. It was found that the order of addition of the reactants on the catalyst has no effect on the N-formylation reactions.

Table 1 N-formylation of some primary amines using $\text{CoFe}_2\text{O}_4@\text{SiO}_2$ -PTA as catalyst^a.

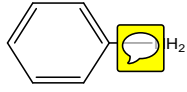
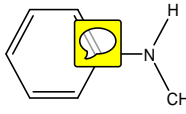
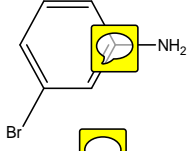
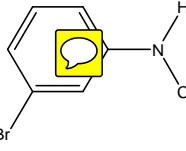
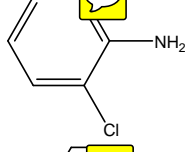
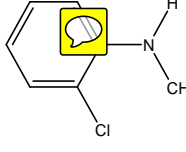

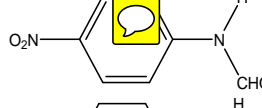

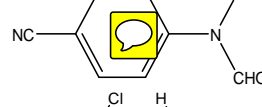
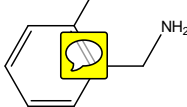
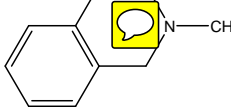
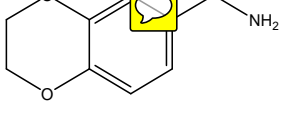


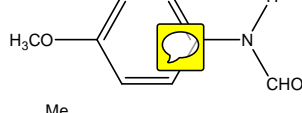
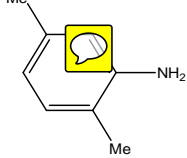
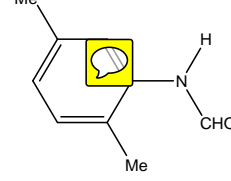
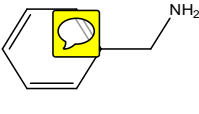
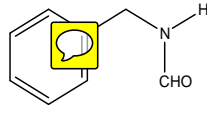
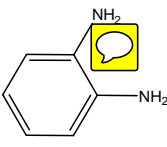
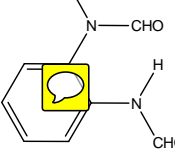
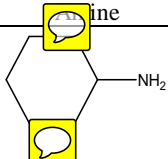
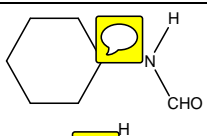
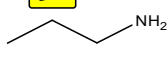
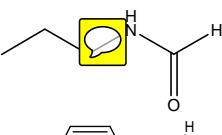
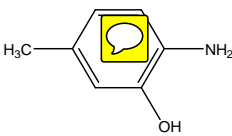
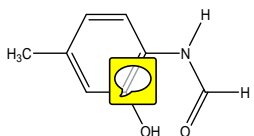
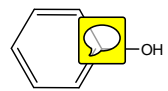
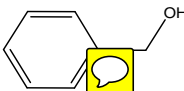
Entry	Amine	Product ^b	Time(min)	Yields (%) ^c
1			30	95
2			35	92
3			35	85
4			60	89
5			50	50
6			45	85
7			60	88
8			25	99
9			35	93
10			35	91
11			60	88 ^d

Table 1(Continued)

Entry	Amine	Product ^b	Time(min)	Yields (%) ^c
12			45	90
13			60	97
14			35	88
15		-	-	-
16		-	-	-

^a Aromatic or aliphatic amine (1 mmol), formic acid (1 mmol), and CoFe₂O₄@SiO₂.PTA(0.05 g) at rt.

^b All the products were identified by spectral data IR with those of authentic samples.

^c Isolated yields

^d amine: formic acid (1:2 mmol)

Our finding, that the –NH₂ group is preferred in these types of reactions than –OH, is in agreement with other previously reported works [39,40]. This can be attributed to nucleophilicities of these functional groups. The –NH₂ group is obviously stronger nucleophile than –OH and therefore no O-formylation reaction is expected.

The effectiveness of the as-synthesized CoFe₃O₄@SiO₂-PTA catalyst in N-formylation reactions is due to presence of PTA in this composite. To further prove this idea, each of CoFe₃O₄, CoFe₃O₄@SiO₂ and neat PTA were examined separately for N-formylation reactions. As seen in Table 2, neither of CoFe₃O₄ or CoFe₃O₄@SiO₂ has shown any catalytic effect on this reaction; whereas neat PTA was found to be as effective catalyst as CoFe₃O₄@SiO₂-PTA. The difficulty in recovery and recycling of pristine PTA, however, limits its application as catalyst for these types of reactions.

Table 2 Comparative study of Catalysts for N-formylation reaction

Entry	Catalysts	Time (min)	Yield%
1	CoFe ₃ O ₄	120	-
2	CoFe ₃ O ₄ @SiO ₂	120	-
3	H ₃ PW ₁₂ O ₄₀	15	91
4	CoFe ₃ O ₄ @SiO ₂ - PTA	30	95

In order to illustrate the merit of the present catalytic system, we compared the results of CoFe₃O₄@SiO₂-PTA in the N-formylation of aniline with formic acid to other reported protocols (see Table 3). Our newly synthesized three-component nanocomposite is an equally or more efficient catalyst than previously reported ones with respect to reaction time and reaction conditions. The superiority of the introduced catalyst in the present work will be more obvious if its magnetic property is taken into account. This magnetically-responsive catalyst can be readily separated from solution by applying an external magnetic field.

Table 3 Comparison of efficiency of various conditions in the N-formylation of aniline.

Entry	catalyst	Time (min)	Temperature (°C)	Yield%	Ref.
1	HClO ₄ -SiO ₂	15	room	96	57
2	^b TiO ₂ -P25	45	room	99.2	58
3	ZnCl ₂	10	70	96	36
4	Silica sulfuric acid	7	50-60	99	56
5	CoFe ₃ O ₄ @SiO ₂ - PTA	30	Room	95	a

a) This work. ^b aniline:formic acid ratio 3:1, in CH₃CN.

3.3. Recycling of the catalyst

The reusability of the catalysts is crucial in the practical application and has to be considered in heterogeneous process. Therefore, reusability of the $\text{CoFe}_2\text{O}_4@\text{SiO}_2\text{-PTA}$ catalyst was investigated. For this purpose, the same model reaction was again examined under optimized conditions. After completion of the N-formylation of aniline, the catalyst was collected by an external magnet, followed by washing it for three times with ethyl acetate. After drying the isolated catalyst at $100\text{ }^\circ\text{C}$ for 2 h, it was reused in a new reaction. As shown in Fig 6, the recovered catalyst could be reused for at least five successive times without any significant loss of its activity. The FT-IR spectrum of the recovered catalyst showed no change after it has been used for four successive times (see Fig.7). Furthermore, the amount of PTA was measured in the recycled catalyst by ICP-AES analysis. This measurement showed that the PTA content of the recycled $\text{CoFe}_2\text{O}_4@\text{SiO}_2\text{-PTA}$ catalyst, after 5 runs, is $0.0823\text{ mmol g}^{-1}$. This indicates the loss of only 6% of the original PTA in the composite.

Leaching test can further confirm the heterogeneous nature of as-fabricated catalyst. Therefore, reaction of aniline and formic acid was carried out in the presence of $\text{CoFe}_2\text{O}_4@\text{SiO}_2\text{-PTA}$ for 15 min under the same used conditions. At this point, the catalyst was removed by applying a permanent magnet and the residue was then allowed to react in the absence of catalyst. No significant conversion of the reactants to the N-formylated product was observed after 3 h of stirring the mixture. These observations clearly rule out the simple contribution of leached homogeneous catalyst in the reaction. The obtained results showed that the designed magnetically-responsive catalyst is economic, easily made and environmentally friendly because of its low leaching after at least five cycles.

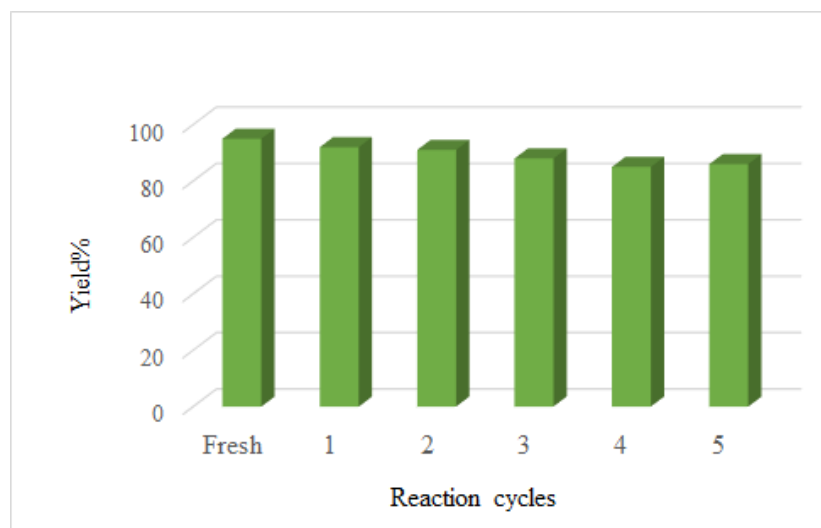


Fig. 6 Reusability of $\text{CoFe}_2\text{O}_4@\text{SiO}_2\text{-PTA}$ catalyst in the model reaction

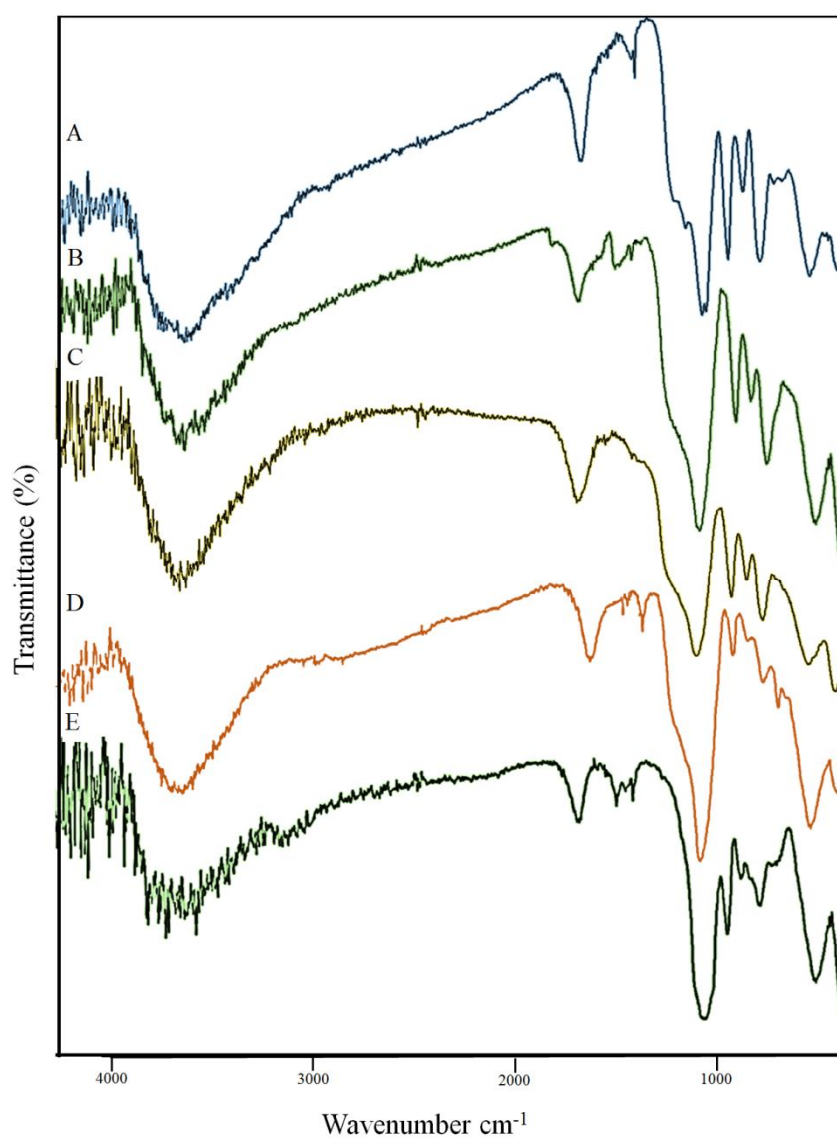
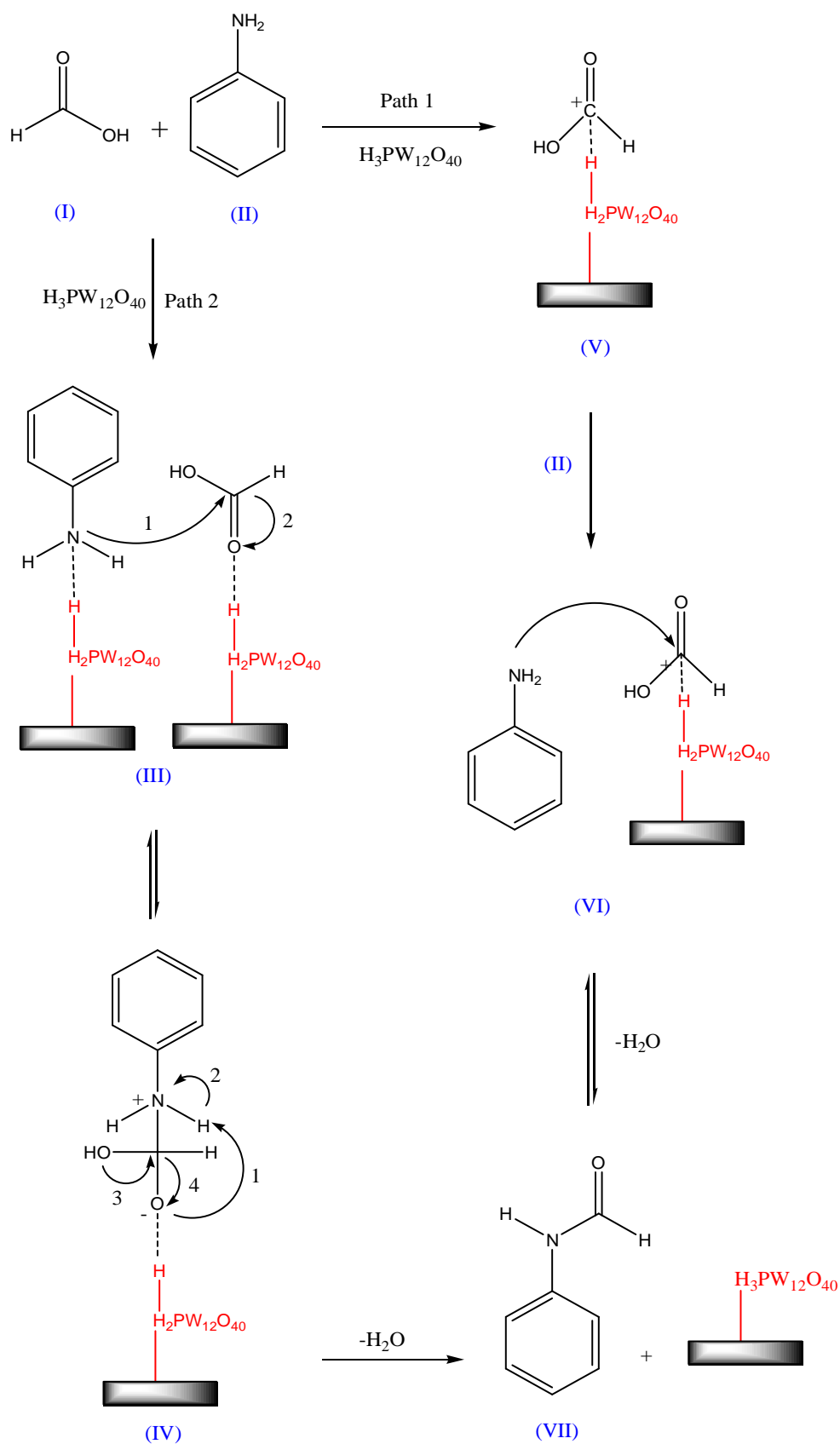


Fig. 7 FT-IR spectra of catalyst: fresh (A) and recycled catalyst after first to fourth runs (B-D)..

3.4. Proposed mechanism for N-formylation of aniline

Based on the previously reported studies [58-61] and our observations in the course of this reaction, the following mechanism, which is consisted of two pathways, can be proposed (see Scheme 3). According to this mechanism; in path 1 the carbonyl group of formic acid is first activated by coordination to PTA on the surface of $\text{CoFe}_2\text{O}_4@\text{SiO}_2$ -PTA catalyst to produce intermediate (v). In fact, formic acid is much weaker Brønsted acid ($K_a=1.77\times 10^{-4}$) than PTA (super-strong acid) and acts as a base in contact with PTA. The activated carbonyl center of intermediate (V) subsequently reacts with the $-\text{NH}_2$ group of aniline to give intermediate (VI) followed by a proton transfer to the catalyst yielding the corresponding formamide (VII). In path 2, on the hand, both formic acid and aniline are coordinated to PTA to form intermediate (III) which then produces intermediate (IV). The later undergoes some rearrangement and proton transfer to give the final N-formylated product.



Scheme 3. Proposed mechanism for N-formylation of aniline on the surface of $\text{CoFe}_2\text{O}_4@\text{SiO}_2$.PTA catalyst

Conclusion

In this study, a new magnetically-responsive composite, $\text{CoFe}_2\text{O}_4@\text{SiO}_2\text{-PTA}$, has been prepared via a simple and rapid procedure. This catalyst was used in some N-formylation reactions which gave high yields of formamides in short reaction times. This chemoselective catalytic reaction was performed under solvent-free conditions so no harmful volatile solvent is released into the environment and can be considered as "Green procedure". This new catalyst has a magnetic core and therefore can be readily separated from the reaction mixture to be reused for several times with high efficiency.

Acknowledgment

The authors wish to acknowledge the support of this work (grant No.1393) provided by the Research Council of Shahid Chamran University, Ahvaz, Iran.

References

- [1] A. Kumar, P. Singh, S. Kumar, R. Chandra, S. Mozumdar, J. Mol. Catal. A: Chem. 276 (2007) 95-101.
- [2] A. Ciftci, D. Varisli, C.K. Tokay, N.A. Sezgi, T. Dogu, Chem. Eng. J. 207-208 (2012) 85-93.
- [3] R.T. Carr, M. Neurock, E. Iglesia, J. Catal. 278 (2011) 78-93.
- [4] M. H. Bhure, I. Kumar, A. D. Natu, R. C. Chikate, C. V. Rode, Catal. Commun. 9 (2008) 1863-1868.
- [5] G. S. Kumar, M. Vishnuvarthan, M. Palanichamy, V. Murugesan, J. Mol. Catal. A: Chem. 260 (2006) 49-55.
- [6] A. M. I. Inicka, E. Bielanska, L. L. Dobrzynska, A. Bielanski, Appl. Catal. A 421-422 (2012) 91-98.
- [7] N. Y. He, C. S. Woo, H.G. Kim, H.I. Lee, Appl. Catal. A 281 (2005) 167-178.
- [8] T. Okuhara, N. Mizuno, M. Misono, Adv. Catal. 41 (1996) 113-252.

- [9] I. V. Kozhevnikov, *J. Mol. Catal. A: Chem.* 262 (2007) 86-92.
- [10] T. Tagawa, J. Amemiya, S. Goto, *Appl. Catal. A* 257 (2004) 19-23.
- [11] J. Kaur, K. Griffin, B. Harrison, *J.Catal.* 208 (2002) 448-455.
- [12] Z. Obali, T. Dogu, *Chem. Eng. J.* 138 (2008) 548-555.
- [13] H. Kim, J. C. Jung, S. H. Yeom, K. Y. Lee, I. K. Song, *J. Mol. Catal. A: Chem.* 248 (2006) 21-25.
- [14] B.S. Li, W. Ma, J.J. Liu, C.Y. Han, S.L. Zuo, X.F. Li, *Catal. Commun.* 13 (2011) 101-105.
- [15] X.M. Yan, P. Mei, J.H. Lei, Y.Z. Mia, L. Xiong, L.P. Guo, *J. Mol. Catal. A: Chem.* 304 (2009) 52-57.
- [16] Y. Kamiya, T. Okuhara, M. Misono, A. Miyaji, K. Tsuji, T. Nakajo, *Catal. Surv. Asia* 12 (2008) 101-113.
- [17] G. S. Armatas, G. Bilis, M. Louloudi, *J. Mater. Chem.*, 2011 (21) 299-302.
- [18] R. M. Ladera, J. L. G. Fierro, M. Ojeda, S. Rojas, *J. Catal.* 312 (2014) 195-203.
- [19] A. P. Philipse, M. P. B. V. Bruggen, C. Pathmamanoharan, *Langmuir* 10 (1994) 92-99.
- [20] Y. Sun, L. Duan, Z. Guo, Y. D. Mu, M. Ma, L. Xu, Y. Zhang, N. Gu, , *J. Magn. Magn. Mater.* 285(2005) 65-70.
- [21] J. Toufaily, M. Soulard, J. L. Guth, J. Patarin, L. Delmote, T. Hamieh, M. Kodeih, D. Naoufal, H. Hamad, *Colloids Surf. A* 316 (2008) 285-291.
- [22] M. Q. He, A.X. Pan, J. M. Xie, D. Li Jiang, X. H. Yuan, M. Chen, *React. Kinet. Mech. Cat. Lett.* 108(2013) 531-544.
- [23] A. Kukovecz, Z. Balogi, Z. Konya, M. Toba, P. Lentz, S.I. Niwa, F. Mizukami, A. Molnar, J. B. Nagyc, I. Kiricsi, *Synthesis, Appl. Catal., A* 228 (2002) 83-94.

- [24] B. Samani Ghaleh Taki, V. Mirkhani, I. M. Baltork, M. Moghadam, Sh. Tangestaninejad, M. Rostami, A. R. Khosropour, J. Inorg. Organomet. Polym. 23 (2013) 758-765.
- [25] X. Feng, G. Y. Mao, F. X. Bu, X. L. Cheng, D. M. Jiang, J. S. Jiang, J. Magn. Magn. Mater. 343 (2013) 126-132.
- [26] J. Tasca, A. Lavat, K. Nesprias, G. Barreto, E. Alvarez, N. Eyler, A. Canizo, J. Mol. Catal. A: Chem. 363 (2012) 166-170.
- [27] V. Polshettiwar, R. Luque, A. Fihri, H. Zhu, M. Bouhrara, J. M. Basset, Chem. Rev. 111 (2011) 3036-3075.
- [28] S. Amiri, H. Shokrollahi, Mater. Sci. Eng. C 33 (2013) 1-8.
- [29] C. Cannas, A. Ardu, A. Musinu, D. Peddis, G. Piccaluga, Chem. Mater. 20 (2008) 6364-6371.
- [30] Y. Deng, D. Qi, C. Deng, X. Zhang, D. Zhao, J. Am. Chem. Soc. 130 (2008) 28-29.
- [31] R. B. N. Baig, R. S. Varma, Chem. Commun. 49 (2013) 752-770.
- [32] X. Zheng, L. Zhang, J. Li, S. Luo, J. P. Cheng, Chem. Commun. 47 (2011) 12325-12327.
- [33] L. Zhao, Y. Chi, Q. Yuan, N. Li, W. Yan, X. Li, J. Colloid Interface Sci. 390 (2013) 70-77.
- [34] X. Q. Chen, M. Arruebo, K. L. Yeung, Catal. Today 204 (2013) 140-147.
- [35] A. Khojastehnezhad, M. Rahimizadeh, F. Moeinpour, H. Eshghi, M. Bakavoli, C. R. Chimie 17 (2014) 459-464.
- [36] A. C. Shekhar, A. R. Kumar, G. Sathaiah, V. L. Paul, M. Sridhar, P. S. Rao, Tetrahedron Lett. 50 (2009) 7099-7101.
- [37] S. Farhadi, M. Zaidi, J. Mol. Catal. A: Chem. 299 (2009) 18-25.

- [38] B. Das, M. Krishnaiah, P. Balasubramanyam, B. Veeranjanyulu, D. N. Kumar, *Tetrahedron Lett.* 49 (2008) 2225-2227.
- [39] M. Lei, L. Maa, L. Hua, *Tetrahedron Lett.* 51 (2010) 4186-4188.
- [40] L. Ma'mani, M. Sheykhan, A. Heydari, M. Faraji, Y. Yamini, *Appl. Catal., A*: 377 (2010) 64-69.
- [41] M. Kooti, M. Afshari, *Mater. Res. Bull.* 47 (2012) 3473-3478.
- [42] H. Hamadi, M. Kooti, M. Afshari, Z. Ghiasifar, N. Adibpour, *J. Mol. Catal. A: Chem.* 373 (2013) 25-29.
- [43] J. C. Bailar Jr., H. S. Booth, M. Grennert, *Inorg. Synth.* 1 (1939) 132-133.
- [44] K. Maaz, A. Mumtaz, S.K. Hasanain, A. Ceylan, *J. Magn. Magn. Mater.* 308 (2007) 289-295.
- [45] W. Stöber, A. Fink, *J. Colloid Interface Sci.* 26(1968) 62-69.
- [46] M. Ma, Y. Zhang, W. Yu, H.Y. Shen, H. Zhang, N. Gu, *Colloids Surf. A* 212 (2003) 219-226.
- [47] H. Ono, T. Katsumata, *Appl. Phys. Lett.* 78 (2001) 1832-1834.
- [48] T. Rakjumar, G.R. Rao, *J. Chem. Sci.* 120 (2008) 587-594.
- [49] B. D. Cullity, 2nd ed. Addison-Wesley, London, 1978.
- [50] M. Kuzminska, T. V. Kovalchuk, R. Backov, E. M. Gaigneaux, *J. Catal.* 320 (2014) 1-8.
- [51] N. A. Comelli, L. M. Grzona, O. Masini, E. N. Ponzi, M. I. Ponzi, *J. Chil. Chem. Soc.*, 49 (2004) 245-250.
- [52] X. Yan, J. Chen, Q. Xue, P. Miele, *Microporous Mesoporous Mater.* 135 (2010) 137-142.
- [53] H. Wang, J. Huang, L. Ding, D. Li, Y. Han, *Appl. Surf. Sci.* 257 (2011) 7107-7112.
- [54] Y. Xiong, Z. Zhang, X. Wang, B. Liu, J. Lin, *Chem. Eng. J.* 235 (2014) 349-355.

- [55] K. P. Dhake, P. J. Tambade, R.S. Singhal, B. M. Bhanage, Green Chem. Lett. Rev. 4 (2011) 151-157.
- [56] D. Habibi, P. Rahmani, Z. Akbaripanah, J. Chem. 2013 (2013) 1-6.
- [57] M. I. Ansari, M. K. Hussain, N. Yadav, P. K. Gupta, K. Hajela, Tetrahedron Lett. 53 (2012) 2063-2065.
- [58] B. Krishnakumar, M. Swaminathan, J. Mol. Catal. A: Chem. 334 (2011) 98-102.
- [59] C. J. Gerack, L.M.White, Molecules, 19 (2014) 7689-7713.
- [60] S.Majumdar, J. De, J. Hossain, A. Basak, Tetrahedron Letters 54 (2013) 262-266.
- [61] D. Wei, C. Cui, Z. Qua, Y. Zhu, M. Tang, J. Mol. Struc-THEOCHEM 951 (2010) 89-92.

Figure Captions

Scheme 1. N-formylation of amine in the presence of $\text{CoFe}_2\text{O}_4@\text{SiO}_2\text{-PTA}$.

Scheme 2. Step - by- step synthesis of $\text{CoFe}_2\text{O}_4@\text{SiO}_2\text{-PTA}$ nanocomposite.

Scheme 3. Proposed mechanism for N-formylation of aniline on the surface of $\text{CoFe}_2\text{O}_4@\text{SiO}_2\text{-PTA}$ catalyst.

Fig. 1. FT-IR spectra of PTA (A), $\text{CoFe}_2\text{O}_4@\text{SiO}_2\text{-PTA}$ (B), $\text{CoFe}_2\text{O}_4@\text{SiO}_2$ (C) and CoFe_2O_4 (D).

Fig. 2. XRD patterns of CoFe_2O_4 (A), $\text{CoFe}_2\text{O}_4@\text{SiO}_2$ (B), $\text{CoFe}_2\text{O}_4@\text{SiO}_2\text{-PTA}$ (C) and PTA(D).

Fig. 3. SEM image of CoFe_2O_4 (A), $\text{CoFe}_2\text{O}_4@\text{SiO}_2$ (B), $\text{CoFe}_2\text{O}_4@\text{SiO}_2\text{-PTA}$ (C).

Fig. 4. EDX spectrum of $\text{CoFe}_2\text{O}_4@\text{SiO}_2\text{-PTA}$ nanocomposite.

Fig. 5. Hysteresis loops of CoFe_2O_4 (A), $\text{CoFe}_2\text{O}_4@\text{SiO}_2$ (B) and $\text{CoFe}_2\text{O}_4@\text{SiO}_2\text{-PTA}$ (C).

Fig. 6 Reusability of $\text{CoFe}_2\text{O}_4@\text{SiO}_2$ -PTA catalyst in the model reaction.

Fig. 7 FT-IR spectra of catalyst: fresh (A) and recycled catalyst after first to fourth runs (B-D).

Table Captions

Table 1 N-formylation of some primary amines using $\text{CoFe}_2\text{O}_4@\text{SiO}_2$ -PTA as a catalyst^a.

Table 2 Comparative study of Catalysts for N-formylation reaction.

Table 3 Comparison of efficiency of various conditions in the N-formylated of aniline.